FIELD ANALYSIS OF MILLIMETER-WAVE GAAS DOUBLE-DRIFT IMPATT DIODE IN THE TRAVELLING-WAVE MODE*

Yoshiro Fukuoka and Tatsuo Itoh

The Department of Electrical Engineering
The University of Texas at Austin
Austin, Texas 78712

ABSTRACT

An analysis of a realistic model of distributed IMPATT structures is described. Wave equations are solved with all losses included. The results show that net gain is produced at frequencies just above the avalanche resonance, while the propagation becomes slow at high frequencies. The results compare favorably with experiment.

INTRODUCTION

An IMPATT diode is an attractive source at millimeter-wave frequencies because of its feasibility of producing a large power. However, as frequencies become higher, it tends to be difficult to use sufficient device area mainly because thinner depletion layer is required for IMPATT operation. A travelling-wave structure is one way of efficiently utilizing larger area of the device [1-3]. The electromagnetic wave travelling along pn junction draws some energy out of dc current and is therefore amplified.

The most elaborate theoretical treatment of such a structure so far was done by Franz et al. [4]. However, their model was still too simplified because inactive layers were all assumed to be perfect conductors and the avalanche region in the depletion layer was assumed to be infinitesimally thin. At mm-wave frequencies, however, the effect of the finite conductivities of these inactive regions is important. They contribute to loss and affect phase constants of the device.

In the present work, a complete set of differential equations governing both wave propagation and avalanche multiplication is solved with boundary conditions including the finite conductivities of the metal contacts. Small-signal assumption is made, and results are presented for a GaAs double-drift IMPATT diode. Computed gain and propagation constants are compared with experimental results published by other authors. They are qualitatively in agreement.

*This work was supported in part by the Joint Service Electronics Program under Grant F49620-82-0033 and in part by the U.S. Army Research Office under Contract DAAG29-81-K-0053.

THEORY

The structure to be studied is a one dimensional multilayered waveguide (Fig. 1), where materials change only in the x direction. In the figure, if a single-drift diode is considered, two center regions (n and p) should be replaced with a single material. In such a structure the dominant propagating mode is a TM mode, which has only the y component of magnetic field and the x and z components of electric field. The expressions of these components in the inactive regions are obtained in a usual way.

In the IMPATT medium, the governing differential equations are as follows [4,5]:

$$\nabla^2\vec{E} - \nabla(\nabla\cdot\vec{E}) - \mu\varepsilon\frac{\partial^2\vec{E}}{\partial t^2} - \mu\frac{\partial\vec{J}_c}{\partial t} = 0$$

$$\nabla\cdot\vec{E} = \frac{q}{\varepsilon}(N_D - N_A + p - n)$$

$$\frac{\partial n}{\partial t} = \frac{1}{q}(\nabla\cdot\vec{J}_n + \alpha|J_n| + \beta|J_p|)$$

$$\frac{\partial p}{\partial t} = \frac{1}{q}(-\nabla\cdot\vec{J}_p + \alpha|J_n| + \beta|J_p|) \qquad (1)$$

where

E : electric field
J_c : conduction current density
J_n : electron current density
J_p : hole current density
N_D : donor concentration
N_A : acceptor concentration
n : electron concentration
p : hole concentration
α : generation rate for electrons
β : generation rate for holes
q : unit charge
ε : permittivity
μ : permeability

Each variable quantity is decomposed into dc and ac (or rf) parts and solved separately. For example,

$$E_x = E_{xDC} + \tilde{E}_x e^{j\omega t-\gamma z}$$

It is reasonable to consider that only x-component of dc electric field exists, therefore dc equations are solved in a similar way as presented by Misawa [6]. This also determines the thickness of the space-charge region (active region). Using the solution of dc equations, ac equations are solved with boundary conditions which require H_y and E_z to be continuous at each boundary.

RESULTS

The parameters chosen for the numerical calculations are shown in Table 1. The structure consists of 8 layers and is very similar to the one used in the experiments made by Bayraktaroglu et al. [7].

The computed results for gain and propagation constants are presented in Figs. 2 and 3, respectively. As frequency becomes lower and approaches to the avalanche resonance, gain increases and the wave propagation becomes faster. In these figures, dotted lines indicate the results for the special case that the depletion region is replaced by a lossless material. Propagation becomes slow wave in this case. Each curve asymptotically approaches to the dotted line at high frequencies, since the device deviates from the IMPATT operation.

Fig. 4 shows the comparison of the present theory and the experimental results obtained in [7]. The device was used as an oscillator with one end open and the other short. In the figure, white dots (o) show the actual device lengths and the oscillation frequency obtained in the experiment, and black dots (•) show one-third of the actual device length (i.e., they are considered to be oscillating at three-quarter wavelength). Three solid curves indicate the theoretical quarter wavelength where net gain is produced in the device. They are in good agreement except two black dots where higher order resonance ($3\lambda/4$) takes place and the actual terminating condition might be more prominent to affect the oscillation frequencies.

Finally, Fig. 5 shows how gain changes with respect to the dc current. As the dc current increases, the gain also increases but suddenly goes to a large loss at certain point. This fact qualitatively agrees with the results of power measurements for the conventional IMPATT diodes [8].

CONCLUSION

Wave propagation phenomena in the travelling-wave IMPATT diode were analyzed numerically, and reasonable results were obtained. It was shown that the propagation was slow wave at high frequencies, but became fast as approaching to the avalanche resonance of the IMPATT medium. The mechanism of producing the fast wave is not yet clear, and investigation is currently being made.

REFERENCES

1. T.A. Midford and H.C. Bowers, "A Two-Port IMPATT Diode Travelling Wave Amplifier," Proc. IEEE, pp. 1724-1725, Oct., 1968.

2. N.S. Davydova, Yu. Z. Danyushevskiy and L.I. Telyatnikov, "Linear Theory of an IMPATT Diode Distributed Microwave Amplifier," Telecommun. Radio Eng., Vol. 27, No. 8, pp. 112-115, Aug., 1972.

3. K.G. Hambleton and P.N. Robson, "Design Consideration for Resonant Travelling Wave IMPATT Oscillators," Int. J. Electronics, Vol. 35, No. 2, pp. 225-244, 1973.

4. M. Franz and J.B. Beyer, "The Travelling-Wave IMPATT Mode," IEEE Trans. Microwave Theory Tech., Vol. MTT-25, No. 11, pp. 861-865, Nov., 1978.

5. D.L. Scharfetter and H.K. Gummel, "Large-Signal Analysis of a Silicon Read Diode Oscillator," IEEE Trans. Electron Devices, Vol. ED-16, No. 1, pp. 64-77, Jan., 1969.

6. T. Misawa, "Negative Resistance in p-n Junctions Under Avalanche Breakdown Conditions, Part II," IEEE Trans. Electron Devices, Vol. ED-13, No. 1, pp. 143-151, Jan., 1966.

7. B. Bayraktaroglu and H.D. Shih, "Millimeter-Wave GaAs Distributed IMPATT Diodes," IEEE Electron Devices Lett., Vol. EDL-4, No. 11, pp. 393-395, Nov., 1983.

8. B. Bayraktaroglu and H. D. Shih, "Integral Packaging for Millimeter-Wave GaAs IMPATT Diodes Prepared by Molecular Beam Epitaxy," Electron. Lett., Vol. 19, No. 9, pp. 327-328, Apr., 1983.

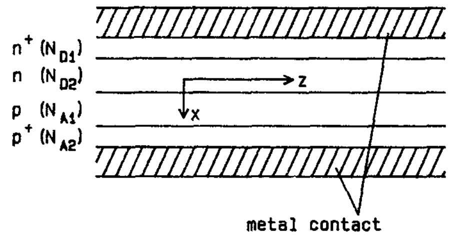

Fig. 1 Side view of travelling-wave double-drift IMPATT diode

Table I Parameters used in numerical calculations

material	thickness	doping level	conductivity
Au	7.0 μm	-	4.3×10^7 S/m
Ti	0.1	-	1.8×10^6
n+ GaAs	0.2	$5.0\times10^{18}/cm^3$	6.81×10^5
n GaAs	0.3	1.5×10^{17}	2.04×10^4
p GaAs	0.3	1.5×10^{17}	9.61×10^2
p+ GaAs	0.2	5.0×10^{18}	3.20×10^4
Ti	0.1	-	1.8×10^6
Au	7.0	-	4.3×10^7

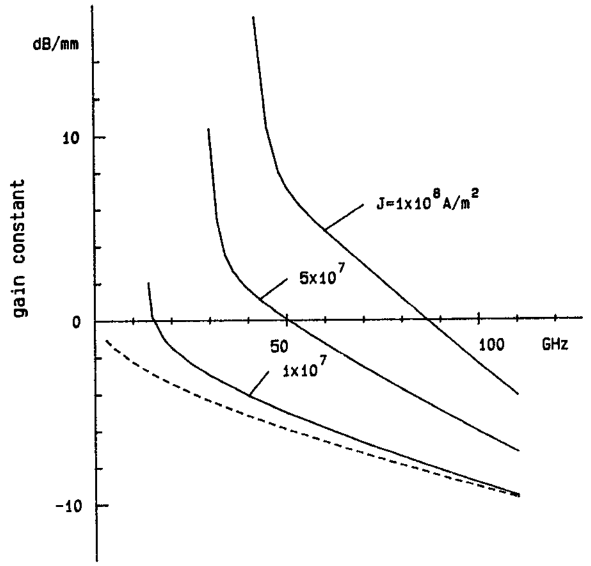

Fig. 2 Gain versus frequency : Curves are shown for 3 different DC current densities.
: Active region is replaced by a lossless material.
: $\sqrt{\varepsilon_r}\, k_o$

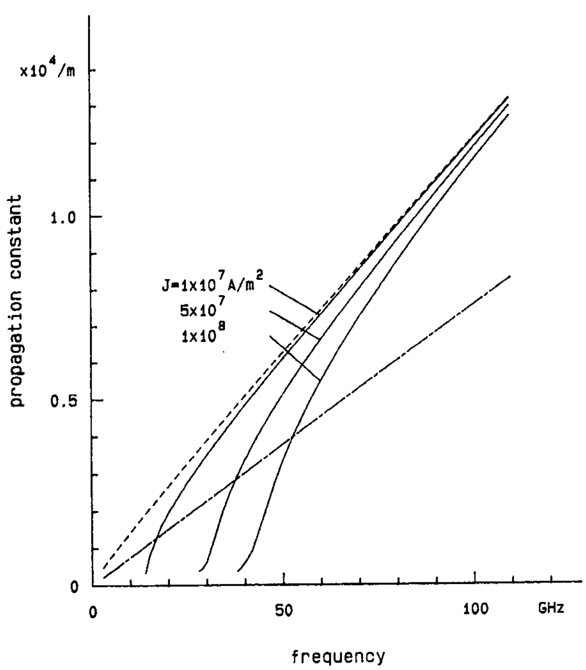

Fig. 3 Propagation constant versus frequency
: Active region is replaced by a lossless material.
: $\sqrt{\varepsilon_r}\, k_o$

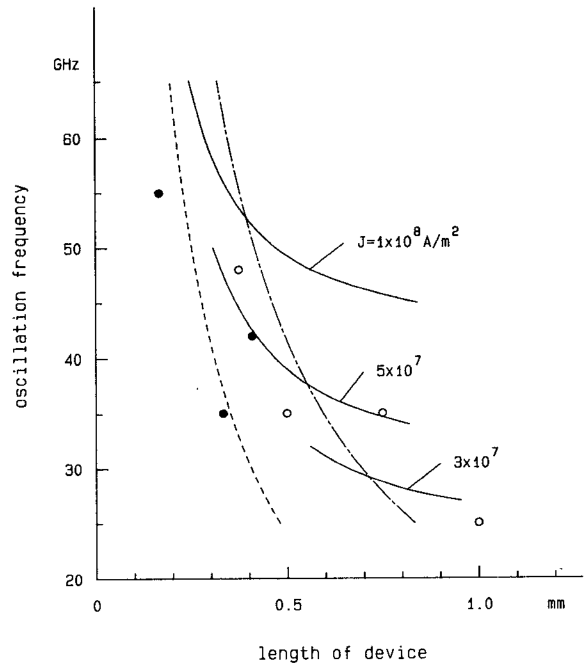

Fig. 4 Oscillation frequency versus length of device : 3 solid curves show theoretical results where net gain is positive.
: experiment (λ/4) [7]
: experiment (3λ/4)
: Active region is replaced by a lossless material.
: $\sqrt{\varepsilon_r}\, k_o$

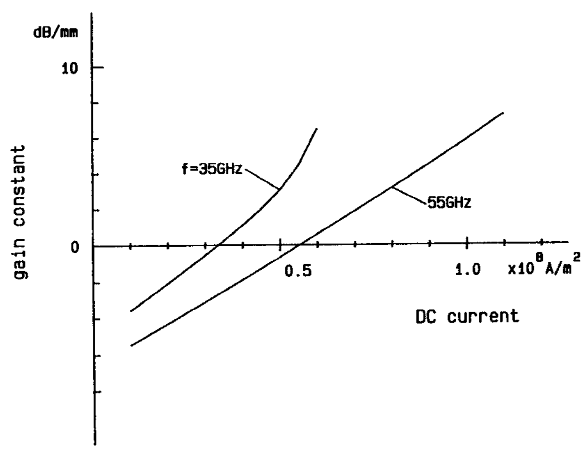

Fig. 5 Gain versus DC current